TRANSFORMING TECHNOLOGY, EXPLORING KNOWLEDGE

Volume 1 Issue 1
Jan 2013 - Mar 2013

ISSN: Applied for

INTERNATIONAL RESEARCH JOURNAL OF ENGINEERING & APPLIED SCIENCES

www.irjeas.com

"FEM Based Prediction of Elastic-plastic Fracture Toughness (*JSZW*) Under Mixed Mode (I/III) Condition"

Sanjay Kumbhare [1], Dr. S. Saxena [2], Rohit Rajvaidhya [3]

[1]*Sanjay Kumbhare, M.Tech final year, Department of Mechanical Engineering, BUIT, Bhopal*
[2]*Rohit Rajvaidya, Asst. Professor, Department of Mechanical Engineering, BUIT, Bhopal*
[3]*Dr. S. Saxena, Sr. Scientist, AMPRI, Bhopal*

***Abstract*- This study aims to predict the elastic-plastic fracture toughness of ductile material using Finite element modeling 'for which we predict the variation of *SZW* and critical *SZW* under mix mode condition and we also use mix mode mixidity. In our findings significant variation in the magnitude of critical *SZW* on the two surfaces were noticed. This is differing in pure mode-I and mode-II. It is due to variation in mode mixidity at different plane levels. Insignificant variations of average critical *SZW* were observed upto 45° (mid thickness) i.e. 45° while, after 45° significant reduction in average critical *SZW* value were observed. In addition, the significant change in sharp crack front of the magnitude of critical *SZW* on two surfaces were observed. Whereas, these changes were varied at different planes. Besides this, the significant variation of sharp crack front (at mid plane) and deformed blunted crack front at critical load line displacement were also observed. In fine, the linear variation of critical *SZW* with initial blunted root radius were observed. It is concluded that the proposed method of *SZW* determination using large deformation FEM analysis can reasonably simulate the process of blunting of the crack tip and can predict the material's *SZW* and *J*-integral value.**

***Keyword*-** *Finite element method, Stretch zone width, Critical stretch zone width, Fracture toughness*

Nomenclature-

A_f	=	Final area of necking cross-section of round tensile specimen
A_0	=	Initial area of cross-section of round tensile strength
B	=	Thickness of fracture specimen
E	=	Modulus of elasticity
$E_{Crit.}$	=	Critical energy density on the material's true stress strain curve
$E_{Fract.}$	=	Fracture energy density on the material's true stress strain curve
K	=	Strength coefficient in a power law material hardening behavior
ε	=	Elastic-plastic true strain
ε_c	=	Critical strain corresponding to onset of necking in tensile specimen
ε_f	=	Fracture strain
σ^*	=	Integral average stress measure on a material's true stress strain curve
σ_f	=	True flow stress
EGF	=	European group of fracture
ASTM	=	American society for testing and materials
CT	=	Compact tension fracture specimen
CTOD	=	Crack tip opening displacement
LLD	=	Load line displacement
SZW	=	Stretch zone width
SZW_c	=	Critical stretch zone width

I. INTRODUCTION

In ductile materials, the pre-existing crack first blunts, subsequently at critical strain, voids are formed ahead of

International Research Journal of Engineering & Applied Sciences
www.irjeas.com, Volume 1, Issue 1, Jan 2013 – Mar 2013, ISSN: Applied for
Page 1-9

the crack tip that finally coalesce with the tip leading to crack propagation [1]. In materials science fracture toughness is a property of which describes the ability of material containing a crack to resist fracture and one of the most important properties of any material for virtually all design application. In modern materials science, fracture mechanics is an important tool in improving the mechanical performance of materials and components. It applies the physics of stress and strain, in particular the theories of elasticity and plasticity, to the microscopic crystallographic defects found in real materials in order to predict the macroscopic mechanical failure of bodies. Fractography is widely used with fracture mechanics to understand the causes of failures and also verify the theoretical failure predictions with real life failures. The current investigation essentially comprises a number of 3D nonlinear FEM simulations to study and correlate crack tip blunting with experimental *SZW, SZWc* and fracture toughness.

II. EXPERIMENTAL DATA

Chemical composition of the material

Chemical compostion of the material is taken from literature in which test had been conducted on SA333Gr6 carbon steel .The chemical composition of the material is show in table 2.1

Material	Base
C	0.14
Mn	0.9
Si	0.25
P	0.016
S	0.018
Al	<0.1
Cr	0.08
Ni	0.05
v	<0.01
N	0.01

Table: 2.1 Chemical compositions in weight %

Fracture toughness Test

Fracture toughness test conducted on Compact tension (CT) specimens of thickness 25 mm and other dimensions conforming to ASTM standard E813-89 have been used for fracture toughness tests. The dimensions of the CT specimens have been shown in Fig. 2.1.

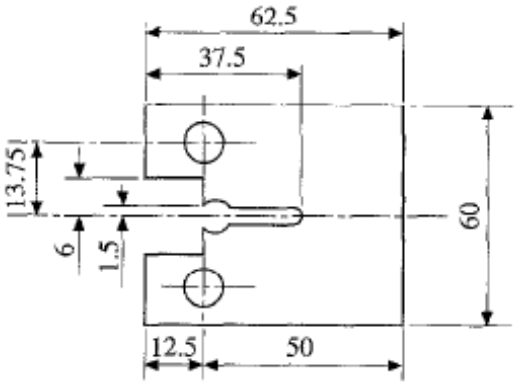

Figure: 2.1 Fracture specimen details

The validity requirements of ASTM E813 for determination of J_{IC} such as regression line, data spacing, and crack shape have been satisfied due to the high toughness of the material. The blunting line equation given by ASTM and that obtained by EGF recommendation has been compared in Fig. 2.2.

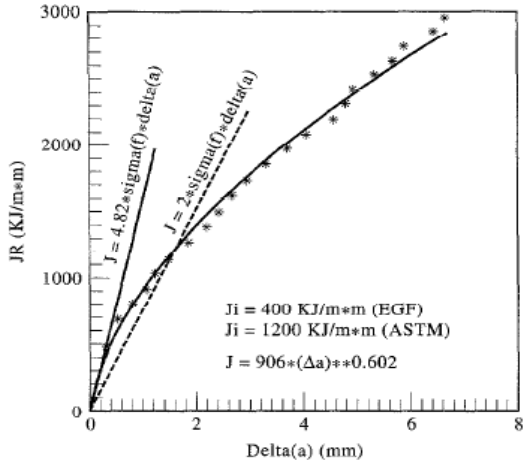

Figure: 2.2 Determination of J_i value using ASTM blunting line equation and EGF blunting line equation.

The Fig 3.4 shows the blunting line equation obtained according to EGF recommendation is suitable for high toughness material. The blunting line equation based on tensile properties has been evaluated according to EGF recommendation. The tensile properties, obtained at same temperature as the fracture toughness test has been conducted, have been used for evaluating the equation of blunting line. The blunting line equation

$$J = \mathrm{m}.\sigma_{\mathrm{f}}.\Delta a \qquad (1)$$

International Research Journal of Engineering & Applied Sciences
www.irjeas.com, Volume 1, Issue 1, Jan 2013 – Mar 2013, ISSN: Applied for
Page 1-9

The fracture toughness J_i value obtained using *EGF* recommendation and critical *SZW* for the material is given Table 2.2

Material	J_i KJ/m²	SZW_c	C_1	C_2
SA333Gr6 Carbon steel	400	193	905.99	.602

Table: 2.2 Experimental fracture properties

For fracture toughness tests *J*-R curves have been established from load line displacement curves and material constants C_1 and C_2 are obtained by fitting a curve using power law equation of the form:

$$J_R = C_1(\Delta a)^{C_2} \qquad (2)$$

Where, Δa is the amount of crack extension in mm and J_R is the material resistance in KJ/m^2. The values of the constants C_1 and C_2 are also shown in Table 2.2 [2-6].

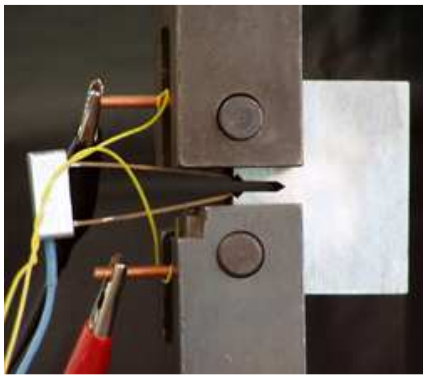

Figure: 2.3 ASTM-1820 Fracture toughness testing and CT specimen

III. FEM SIMULATION

Numerical FEM model

There is an increasing effort to use critical stretch zone width (*SZW*) for the evaluation of initiation fracture toughness that is considered as geometry independent material property. The existing numerical *SZW* evaluation method is based on crack tip opening displacement measurement, which is evaluated using various definitions. This numerical method also does not define the critical stage for critical *SZW* measurement. This work attempts to establish a procedure for numerical determination of *SZW*, its critical value (*SZW*c) and initiation fracture toughness using tensile test data. The proposed methodology also tries to explain the mechanism involved in the creation of stretched zone and thus defines the stage to calculate critical *SZW*. Numerical analyses have also been carried out to understand the role of crack tip constraint in standard fracture specimen during the blunting process and the tensile test sample.

The investigation was limited to CT specimen analysis subjected to mode-I type of loading. To establish the methodology for numerical *SZW* determination, to have better understanding of the variation of fracture parameters across the thickness, one-fourth 3D FEM model of CT specimen have been used [3]. The symmetry in this case permits consideration of only one fourth of the specimen geometry for computational economy. The analyses were done using commercial FEM software ABAQUS [4]. The mesh was constructed with eight nodded brick elements with reduced integration and hourglass control option.

In the mesh convergence study several finite element models having elements size near the crack tip varies from 100 to 5 μm were considered. After the mesh convergence study the element size near the crack front is stick to 10 μm in the radial direction and 5 μm along the blunted crack surface. Such type of initial mesh configuration near the crack tip region helps in keeping good aspect ratio of the elements near the crack tip, during its blunting. In the finite element model 38 040 brick elements were used with 10 elements in the thickness direction. Generally the *SZW* in various engineering materials varies up to 250 μm. Therefore dense mesh is provided up to 250 μm to arrest the steep parameters variation near the crack front. The mesh is further coarsening in the region away from the crack front. The material undergoes a large strain and rotation at the crack tip, which necessitated a constitutive framework based on finite deformation for the numerical simulation. The flow behaviour of the material is assumed to follow the power law

$$\sigma_f = K\varepsilon^n \qquad (3)$$

Where σ_f is the true flow stress, *K* is the strength coefficient ε is the elastic–plastic true strain and *n* is the strain hardening exponent. In the entire simulation power law variation has been used as the input, where *K* and *n* gives the entire material curve. In the study, material's *K* value is derived at a lower strain values to match well the yield strength of the material, whereas *n* value is derived using a log–log plot of true stress–strain

International Research Journal of Engineering & Applied Sciences
www.irjeas.com, Volume 1, Issue 1, Jan 2013 – Mar 2013, ISSN: Applied for
Page 1-9

curve and on an average *n* value will be the best fit. On the whole it is expected to hold well for the full range of strain values. Nonlinear analyses were done considering both geometric and material nonlinearity.

NUMERICAL DETERMINATION

Stretch zone width

In the fracture testing of CT specimen with the increase in load line displacement (LLD) maximum part of plastic energy dissipates near the crack front. In order to demarcate the *SZW* (the highly deformed region) from the other remaining region, it requires defining a critical energy density. Following this the *critical energy density* used to delineate the highly stretched region is defined on the material's true stress–strain curve as the energy density integral at the critical strain (ε_c) corresponding to onset of necking in tensile specimen or strain hardening exponent (*n*) for the specific case of power law variation of material's true stress–strain curve, given as

$$E_{Crit} = \int_0^{\varepsilon_c} \sigma d\varepsilon \qquad (4)$$

The variation of plastic energy density (PED) near the blunted crack front with respect to deformed X-co-ordinates from crack tip with increase in LLD. The above variation is shown at a plane near the mid thickness of the specimen. The region having energy density greater than the critical energy density delineates the stretched region denoted as numerically determined *SZW* and will keep on increasing with LLD. This leads us to understand the 'Stretch zone width' as the zone of intense plastic deformation that corresponds to the onset of material instability considered to be due to the phenomenon associated with necking instability strain. The variation of numerically predicted *SZW* across the thickness resembles very well with the *SZW* variation generally observed in experimental results, thus validating the proposed *SZW* determination methodology. The *SZW* is also assessed by determining CTOD by 45◦ line method. The proposed methodology based *SZW* result near mid plane is compared with half CTOD results measured conventionally (45◦ line method). The stretch zone height (SZH) is also determined considering as Y-deformation of the region where the plastic energy density exceeds the *critical energy density* defined by Eq. (2). It is observed that SZH predicted by proposed energy based method compares well with 45◦ line method whereas for a given LLD, *SZW* predicted by proposed method is on the higher side as compared to conventional (45º line) method. In conventional (45º line) method semicircular blunting shape is always assumed whereas no such assumption is made in the proposed numerical method of *SZW* determination. The validation of proposed methodology of *SZW* determination is also done using the experimental results of fracture toughness and *SZW* value. The numerical fracture toughness *J* can be determined using the following equation:-

$$J = m\sigma^* CTOD = m\sigma^* (2SZW) \qquad (5)$$

where *m* turns out to be a material independent parameter ≈1.25,19 CTOD is the crack tip opening displacement, σ^* is defined on a material true stress–strain curve as the integral average stress measure, given as

$$\sigma^* = \frac{\int_0^{\varepsilon_c} \sigma d\varepsilon}{\int_0^{\varepsilon_c} d\varepsilon} \qquad (6)$$

Here, critical strain (ε_c) is defined as critical strain (ε_c) at onset of necking in tensile specimen equals to strain hardening exponent (*n*) for a specific case of power law variation of true stress–strain material[5]. The experimental variation of blunting slope matches well with numerical results using proposed *SZW* method. Similarly in other cases also it compares well with experimental results. It can also be appreciated that the numerically predicted fracture toughness values using Eq. (3) is on the conservative side as compared to experimental results. The present method can predict well the experimental *SZW* and fracture toughness values.

Critical stretch zone width

With LLD the energy density accumulated near the crack tip increases and reaches a value associated with fracture. It is defined on the true stress–strain material curve as the energy density integral up-to fracture strain $\left[\varepsilon_f = In\left(\frac{A_o}{A_f}\right)\right] \in (\varepsilon_f)$ or the numerically determined strain value in tensile test simulation corresponding to experimental total percentage elongation (if it is greater), obtained in tensile test specimen when fracture occurs, given as

$$E_{Fract.} = \int_0^{\varepsilon_f} \sigma d\varepsilon \qquad (7)$$

International Research Journal of Engineering & Applied Sciences
www.irjeas.com, Volume 1, Issue 1, Jan 2013 – Mar 2013, ISSN: Applied for
Page 1-9

Where $E_{Fract.}$ is the fracture energy density. The above defined fracture energy density is used to determine the critical *SZW* at critical LLD, where the crack initiation occurs in standard fracture specimen. The proposed method of *SZW* determination accurately predicts the trend as well as the magnitude of *SZW*c. This methodology also explains the mechanism involved in the creation of stretch zone thereby defines the stage where to calculate critical *SZW*.

The procedure to numerically predict *SZW* and *SZW*c can be summarized as follows:

1. Plot the variation of plastic energy density with deformed X-co-ordinates w.r.t. crack tip, for the increase in load-line-displacement.
2. Define the *critical* and *fracture energy density* for the material. *Critical energy density* corresponds to the energy density integral up-to necking instability strain or strain-hardening exponent (*n*) for a specific case of power law material hardening behaviour that is obtained by tensile specimen testing. Fracture energy density corresponds to the energy density required to fracture the tensile specimen. Both these energy densities are defined on a true stress–strain material variation, as same material definition is used in FEM analysis.
3. Measure the region (deformed X-co-ordinates) exceeding the material's critical energy density defined by Eq. (2) in the figure drawn in step 1. This deformed X co-ordinate w.r.t. crack tip is *SZW* and it will be a region on blunted crack surface, where the energy density exceeds the critical energy density.
4. The *SZW* measured in step 3 will keep on increasing with LLD until the energy density at the crack front reaches *fracture energy density*. At a critical LLD, *SZW*c is then measured in the region near the mid plane akin to that of experimental method. *SZW*c will be a region on the blunted crack surface, where the energy density varies from *critical* at one end and *fracture energy density* on the other end.[6]

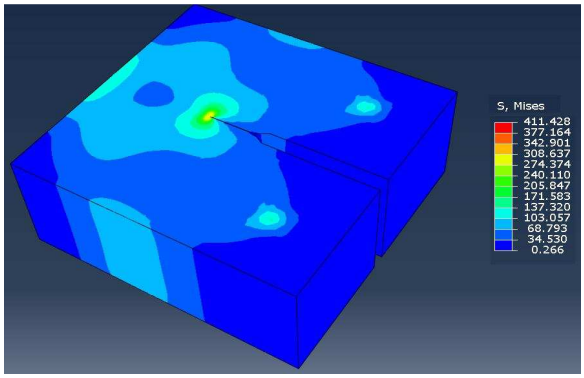

Figure: 3.1 FEM model and result for CT specimen

IV. RESULTS AND DISCUSSION

Variation of *SZW* across the thickness under mixed mode

The average critical *SZW* on the two surfaces converges at the mid thickness of fracture specimen as shown in Graph 4.1.

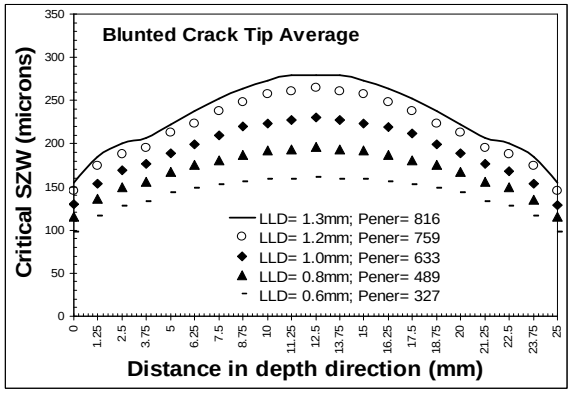

Graph 4.1
Average critical SZW variations under mix mode (15^0 mode mixity)

Variation of *SZW* across the thickness under mixed mode with blunted crack front

The variation of average critical *SZW* values across the fracture specimen thickness is shown in Graph 4.2

International Research Journal of Engineering & Applied Sciences
www.irjeas.com, Volume 1, Issue 1, Jan 2013 – Mar 2013, ISSN: Applied for
Page 1-9

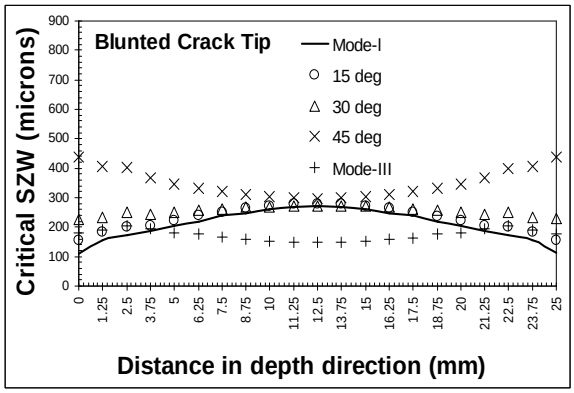

Graph 4.2
Average critical SZW variations on two fracture surfaces using blunted crack front

The variation of average critical *SZW* near the mid thickness is plotted in Graph 4.3.

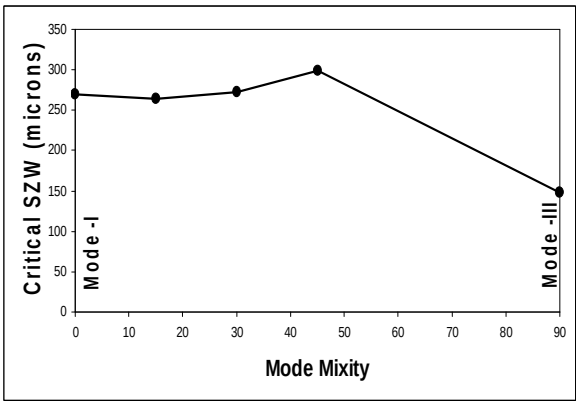

Graph 4.3
Average critical SZW variations with mode mixity using blunted crack front

It can be seen that there is a negligible variation of average critical *SZW* near the mid thickness due to the change in mode mixity upto 45 degree. There is a significant reduction (45%) in average critical *SZW* value under pure mode–III case when compared with mode-I value using blunted crack front.

Variation of *SZW* across the thickness under mixed mode with sharp crack front

The average critical *SZW* on the two surfaces converges at the mid thickness of fracture specimen as shown in Graph 4.4

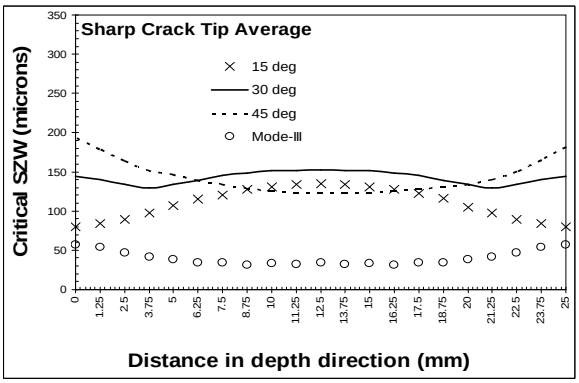

Graph 4.4
Average critical SZW variation on two fracture surfaces using sharp crack front (Considering critical pener 1550/100)

The variation of average critical *SZW* near the mid thickness is plotted in Graph 4.5.

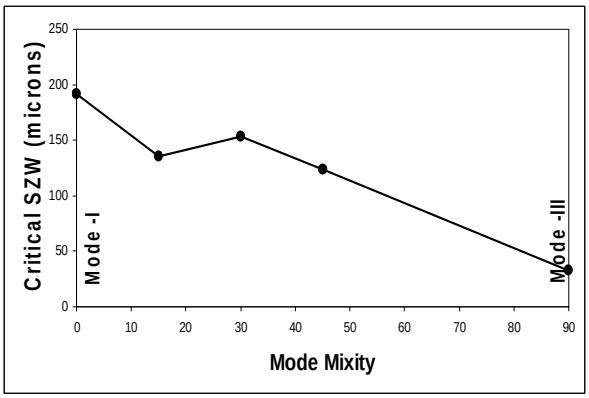

Graph 4.5
Average critical SZW variation with mode mixity using blunted crack front (Considering critical pener 1550/100)

Variation of blunted crack front with mode mixity (initial blunted crack front)

Graph 4.6 showed the variation of initial blunted crack front (at mid plane) and deformed blunted crack front at critical load line displacement where the maximum energy reaches fracture energy of the material.

International Research Journal of Engineering & Applied Sciences
www.irjeas.com, Volume 1, Issue 1, Jan 2013 – Mar 2013, ISSN: Applied for
Page 1-9

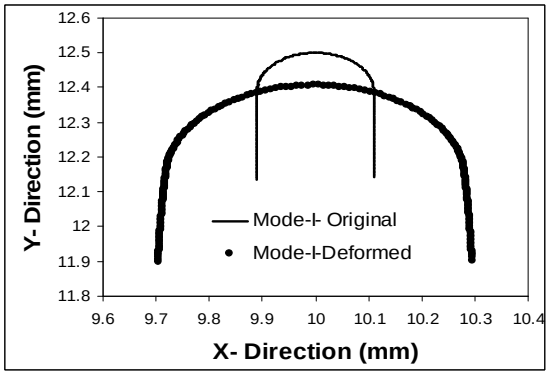

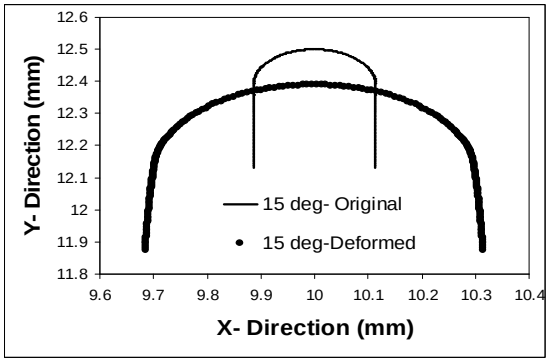

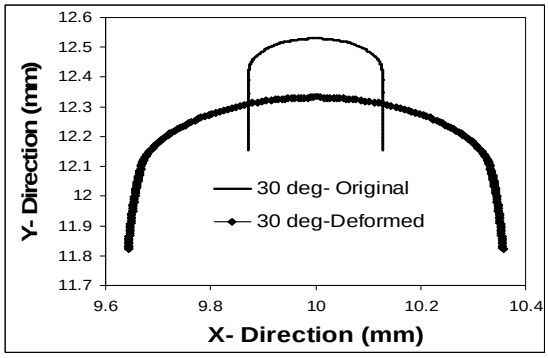

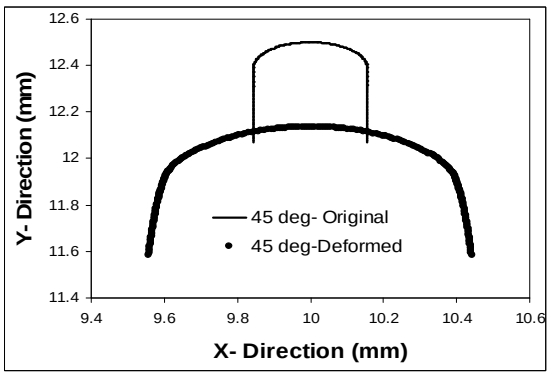

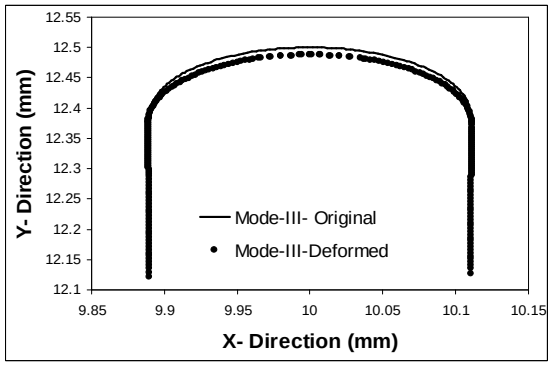

Graph 4.6
Average critical SZW variation with mode mixity using blunted crack front

Variation of mid plane with mode mixity (initial blunted crack front case)

The change of mid plane in the thickness direction along the blunted crack front near the mid thickness is shown in Graph 4.7 and Graph 4.8

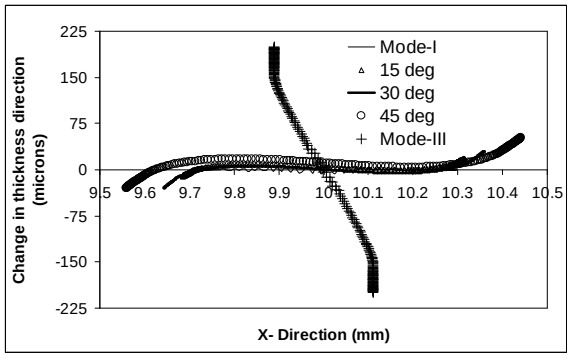

Graph 4.7
Change of mid plane in thickness direction with mode mixity using blunted crack front

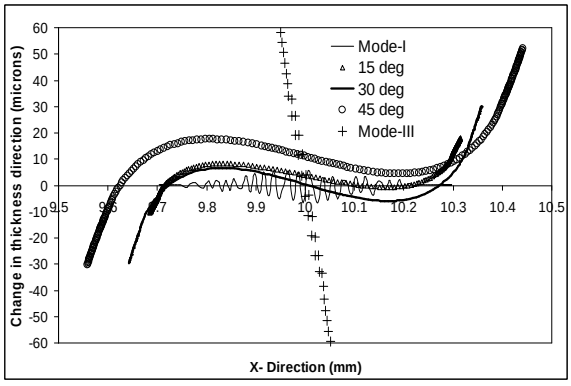

Graph 4.8
Change of mid plane in thickness direction with mode mixity using blunted crack front

From the Graphs, it can be seen with the increase in mode-III contribution, the change in plane increases. There can be a maximum variation of nearly 80 microns magnitude as can be seen in 45^o mode mixity.

Variation of blunted crack front with mode mixity (initial sharp crack front)

Graph 4.9 showed the variation of sharp crack front (at mid plane) and deformed blunted crack front at critical load line displacement where the maximum energy reaches the critical fracture energy of the material.

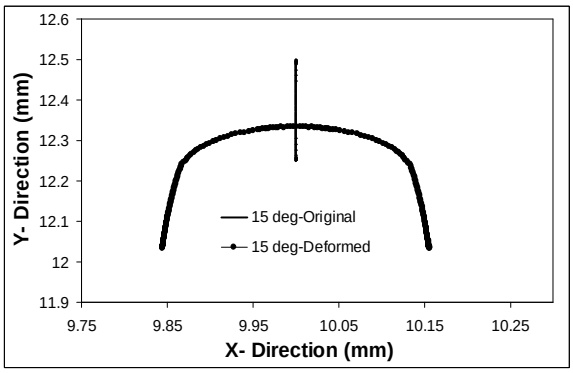

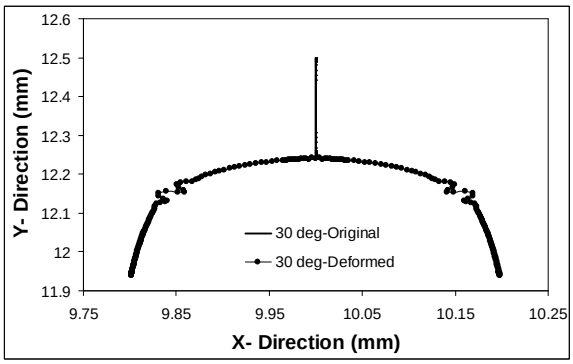

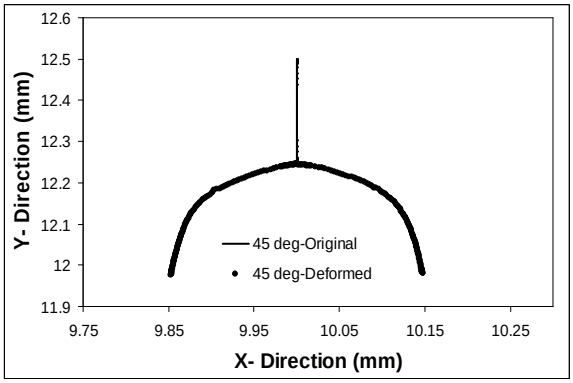

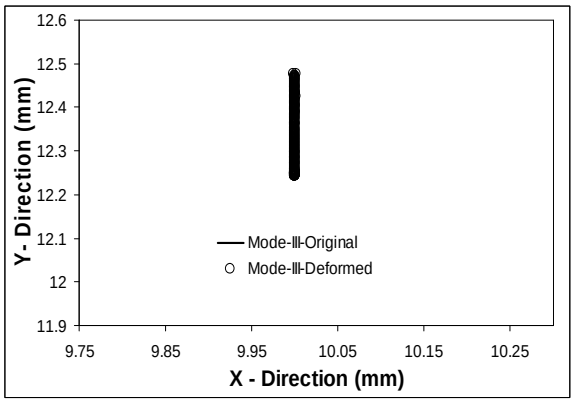

Graph 4.9
Average critical SZW variation with mode mixity using sharp crack front

Variation of mid plane with mode mixity (initial sharp crack front case)

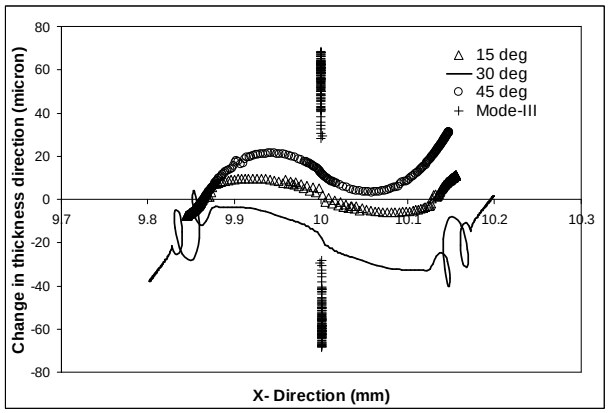

Graph 4.10
Average critical SZW variation with mode mixity using sharp crack front

From the Graphs, it can be seen with the increase in mode-III contribution, the change in plane increases. There can be a maximum variation of nearly 50 microns magnitude as can be seen in 45^o mode mixity.

Variation of critical *SZW* with change in initial blunted root radius

Graph 4.11 showed the average critical *SZW* using different initial blunted crack front.

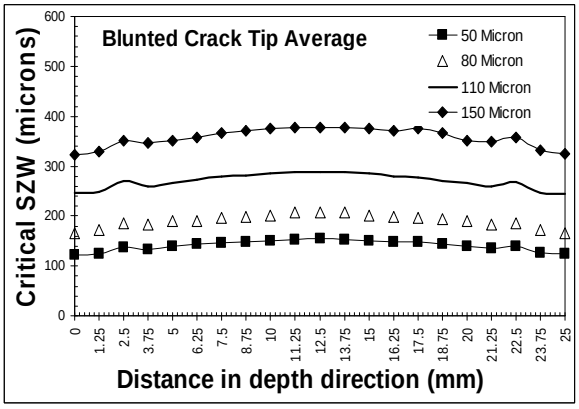

Graph 4.11 (a)
Variation of average critical SZW with root radius

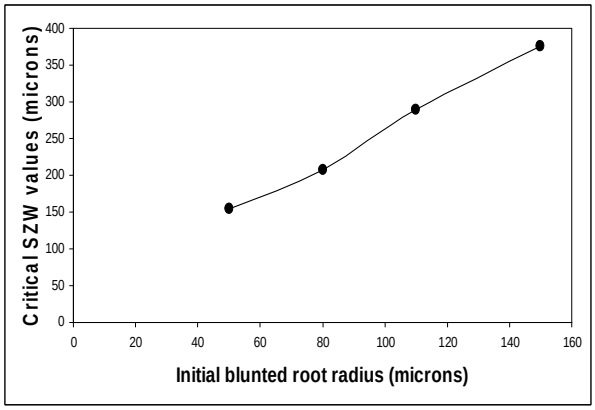

Graph 4.11 (b)
Variation of average critical SZW with root radius

A linear variation of critical *SZW* with initial blunted root radius is seen in the predicted result which matches well with the experimental findings.

VI. CONCLUSION

1. Critical *SZW* on two surfaces varies across the thickness.
2. Critical *SZW* varies with mode mixity both using blunted and sharp crack front.
3. There is change in mid plane under mixed mode fracture.
4. Critical *SZW* is dependent on initial root radius and increase with the increase in initial notch root radius.

VII. REFERENCES

1. AndersonTL. Fracture mechanics fundamental and applications. 2nd ed. CRC press; 1994

2. P.K. Singh, J. Chattopadhyay, H.S. Kushwaha "Tensile and fracture properties evaluation of PHT system piping material of PHWR", International Journal of Pressure Vessels and Piping 75, September 1997, pp 271-280.

3. ABAQUS Version 6.6 (2006) User's manual, Rising Sun Mills Valley Street province, RI.

4. M. Srinivas, G. Malakondaiah, R.W. Armstrong and P. Rama Rao (1991) Ductile fracture toughness of polycrystalline Armo Iron of varying grain size. *ACTa. Mater. 39,807-816.*

5. Sanjeev Saxena, N. Ramakrishnan, J.S. Chouhan, "Establishing methodology to predict fracture behaviour of pipingcomponents", Engineering Fracture Mechanics 77, January 2010, pp 1058–1072

6. R.K.V. Suresh, N. Ramakrishnan, M. Srinivas, and P. Rama Rao, (1999) on the determination of J_{IC} using stretch zone width method.